

Article

Model for Proton Acceleration in Strongly Self-Magnetized Sheath Produced by Ultra-High-Intensity Sub-Picosecond Laser Pulses

Artem V. Korzhimanov ^{1,2} 

¹ Federal Research Center, A. V. Gaponov-Grekhov Institute of Applied Physics, Russian Academy of Sciences, 603950 Nizhny Novgorod, Russia; artem.korzhimanov@ipfran.ru

² Faculty of Radiophysics, Lobachevsky State University of Nizhny Novgorod, 603022 Nizhny Novgorod, Russia

Abstract: Recently, it has been experimentally shown that the sheath acceleration of protons from ultra-thin metal targets irradiated by sub-picosecond laser pulses of intensities above 10^{21} W/cm² is suppressed compared to well-established models. This detrimental effect has been attributed to a self-generation of gigagauss-level quasi-static magnetic fields in expanded plasmas on the rear side of a target. Here we present a set of numerical simulations which support this statement. Based on 2D full-scale PIC simulations, it is shown that the scaling of a cutoff energy of the accelerated protons with intensity deviates from a well-established Mora model for laser pulses with a duration exceeding 500 fs. This deviation is showed to be connected to effective magnetization of the hottest electrons producing at the maximum of the laser pulse intensity. We propose a modification of the Mora model which incorporates the effect of the possible electron magnetization. Comparing it to the simulation results shows that by appropriately choosing a single fitting parameter, the model produces results that quantitatively coincide with simulations.

Keywords: laser plasma interaction; ion acceleration; femtosecond pulse



Academic Editor: Francesco Schillaci

Received: 3 January 2024

Revised: 18 December 2024

Accepted: 10 January 2025

Published: 20 January 2025

Citation: Korzhimanov, A.V. Model for Proton Acceleration in Strongly Self-Magnetized Sheath Produced by Ultra-High-Intensity Sub-Picosecond Laser Pulses. *Quantum Beam Sci.* **2025**, *9*, 4. <https://doi.org/10.3390/qubs9010004>

Copyright: © 2025 by the author. Licensee MDPI, Basel, Switzerland. This article is an open access article distributed under the terms and conditions of the Creative Commons Attribution (CC BY) license (<https://creativecommons.org/licenses/by/4.0/>).

1. Introduction

Laser-plasma sources of high-energy protons and ions can find applications in hadron therapy, the radiography of fields in dense plasma, and the production of neutron beams [1–6]. In particular, recent work has demonstrated a laser-plasma neutron source for neutronography and neutron spectroscopy [7,8]. However, practical applications require a further increase in the brightness of the ion sources as well as the energy of the ions in them. This can be achieved by using more intense and longer laser pulses [9–11]. However, as was shown in a recent paper [12], when using laser pulses with a duration of hundreds of femtoseconds and an intensity of the order of 10^{21} W/cm², the efficiency of laser-plasma ion acceleration drops due to the self-magnetization effect of the expanding plasma. Thus, it is necessary to investigate this effect in more detail and, in particular, to construct models that take it into account.

The most common method of laser-plasma ion acceleration at currently achievable radiation intensities is Target Normal Sheath Acceleration (TNSA) [13]. When a relatively thin—on the order of several microns—solid-state target is exposed to laser radiation with an intensity above 10^{18} W/cm², the effective absorption of laser energy occurs due to the generation of beams of high-energy relativistic electrons thrown deep into the target. These electrons, flying through the target without scattering, fly out from the rear side of the target and create a quasi-static electric field, which ionizes the rear of the target and initiates its expansion. As a result, a plume of the collisionless plasma is formed, in which

electrons are heated to relativistic energies, while ions remain cold and move laminarly, being gradually accelerating.

The Mora model [14] is often used to describe this process. However, it does not take into account the effect of magnetic field generation in the expanding plasma. This magnetic field is generated by a current of high-energy electrons injected by a laser pulse and propagating along the symmetry axis of the system. At high intensities, this field can become so large that it begins, first, to deflect ions, resulting in the formation of a ring-shaped distribution on the detector [15], and second, begins to deflect electrons as well. As a result, the plasma is magnetized, the electrons begin to drift in the magnetic field, their effective velocity drops, and they become unable to reach the expanding front. This effectively reduces the maximum energy of the accelerated ions, which was observed in the experiment [12,16,17].

In this work, a more detailed study of the self-magnetization effect of the expanding plasma cloud is carried out by numerical simulation and a simple model estimation of the magnitude of the generated magnetic field is proposed. This allows to formulate a relatively simple modification of the Mora model, taking into account the self-magnetization effect. The fitting parameters of the modified model are selected by comparison with the results of numerical simulations over a relatively wide range of laser pulse durations and intensities.

2. Methods

2.1. Numerical Simulations

Numerical modeling was carried out by the fully electrodynamic relativistic Particle-In-Cell (PIC) method, which allowed us to solve the closed system of Maxwell's equations for the electromagnetic field and kinetic equations for plasma ions and electrons [18]. Modeling was carried out using the PICADOR software package [19].

A two-dimensional problem was investigated. The width of the modeling region in all calculations was fixed and equal to 80 μm , and the length varied depending on the duration and intensity of the laser pulse in the range from 280 to 480 μm , so that by the end of the laser pulse, plasma did not leave the simulated region. The grid spacing was 20 nm along both axes. Absorbing conditions for particles and fields were used at the boundaries of the modeled region. The simulation time varied from 3 ps to 6 ps depending on the laser pulse duration, with the same time step of 0.02 fs.

The plasma at the initial moment of time was a layer with sharp boundaries with a thickness of 2 μm at a distance of 30 μm from the left boundary of the computational region. The main part of the plasma consisted of aluminum ions Al^{9+} . On the rear side of the aluminum layer, there was a thin (20 nm) layer of hydrogen ions (protons) simulating the natural contamination usually present on the surface of targets in experiments. The plasma density was equal to the natural aluminum density of 2.7 g/cm^3 , corresponding to an electron concentration of $4.5 \times 10^{23} \text{ cm}^{-3}$. The temperature of the electrons and ions at the beginning was 100 eV. The number of particles in the cell at the initial time was 200.

The laser pulse was generated at the left boundary of the computational domain. It had a Gaussian shape in both the longitudinal and transverse directions and was focused on the front surface of the plasma layer normal to it into a spot with a diameter of 4 μm or 1.5 μm at Full Width at Half Maximum (FWHM) of intensity. The pulse duration ranged from 400 fs to 1 ps at FWHM, and its intensity at the focus ranged from $3 \times 10^{19} \text{ W}/\text{cm}^2$ to $3 \times 10^{21} \text{ W}/\text{cm}^2$.

2.2. Mora Model

The Mora model [14] for laser-plasma ion acceleration in the TNSA regime is based on the well-known solution of the problem of the collisionless plasma expansion into

vacuum [20–22]. According to this solution, the ions flying at the front of the expanding cloud have the maximum energy, which grows with time according to the law

$$\varepsilon_i = 2T_e [\ln(2\omega_{pi}\tau)]^2, \quad (1)$$

where T_e is the electron temperature expressed in energy units, ω_{pi} is the ion plasma frequency in an unperturbed plasma, and τ is the time elapsed since the beginning of the expansion.

In the Mora model, it is assumed that T_e is the temperature of the hot fraction of electrons injected into the target by the laser pulse. It is equal to the oscillation energy of the electrons in the laser field and, when calculated carefully, is related to the field amplitude as follows [23]:

$$T_e = m_e c^2 \left(\frac{\pi}{2K(-a^2)} - 1 \right), \quad (2)$$

where m_e is the mass of the electron, c is the speed of light, $K(x)$ is the modified Bessel function of the second kind of the 1st order, and $a = eE/m_e\omega c$ is a dimensionless field amplitude (E is an electric field amplitude, ω is a frequency of laser radiation, and e is the elementary charge). At high intensities, $a \gg 1$, and $T_e \approx am_e c^2$.

As can be seen from Equation (1), the ion energy is mainly determined by the electron temperature. The dependence on the plasma frequency and time is logarithmic and therefore weak, so they can be estimated on an order of magnitude and used as fitting parameters of the model. Thus, the plasma ion frequency can be estimated by assuming that the concentration of thrown-in electrons is approximately equal to the relativistically corrected critical electron concentration $N_e = \gamma N_{cr} = \gamma \varepsilon_0 m_e \omega^2 / e^2$ (ε_0 is the vacuum permittivity, and $\gamma = \sqrt{1 + a^2}$ is a relativistic gamma-factor of electrons in a wave of amplitude a). So we have $\omega_{pi} = (Ze^2 \gamma N_{cr} / \varepsilon_0 m_i)^{1/2} = \omega (Zm_e / m_i)^{1/2} (1 + a^2)^{1/4}$ (Z is an ion charge number, m_i is an ion mass). The acceleration time for sufficiently long laser pulses so that $\omega \tau_L (Zm_e / m_i)^{1/2} \gg 1$ (in practice, this is achieved for pulses of the order of 100 fs or more in duration) is determined mainly by the pulse duration τ_L : $\tau = \tau_L$.

Thus, for sufficiently long and intense laser pulses, the following approximate formula for the cutoff energy of the ion spectrum is obtained:

$$\varepsilon_c = 2a_{max} \left[\ln \left(2\omega \tau_L (Zm_e / m_i)^{1/2} \right) \right]^2, \quad (3)$$

where a_{max} is the maximum field amplitude in the laser pulse. In practice, numerical modeling has shown that this formula gives the correct dependence on the parameters but few times lower than the absolute value of the energy. This difference can be eliminated by introducing a fitting multiplier, the specific value of which depends on the shape of the laser pulse (in the case of a Gaussian pulse—on its focusing diameter and duration) [24,25].

3. Results

3.1. Magnetic Field Generation Model

To estimate the magnitude of the toroidal magnetic field generated in the expanding plasma, consider the following model, schematically depicted in Figure 1. Laser radiation incident on the left boundary of a target with thickness d generates a stream of high-energy electrons traveling to the right and flying in a cone with an opening angle of 2θ . As they fly off the rear edge of the target, they create a toroidal magnetic field [16]. To estimate the magnitude of this field, we consider two limiting cases.

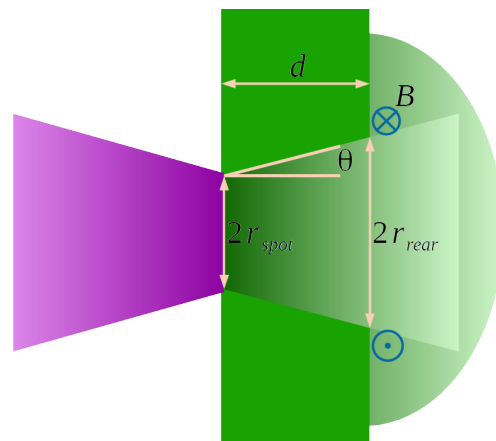


Figure 1. Model of toroidal magnetic field generation. The laser pulse (magenta) interacts with the surface of the target (green) and generates a stream of high-energy electrons flying in a cone with an opening angle of θ . On the rear surface of the target, this current generates a magnetic field B .

At small current densities, its magnetic self-interaction can be considered negligibly small, and then the magnitude of the magnetic field can be estimated by the magnetostatic formula for the cylindrical current. If the concentration of electrons in the flow flying out of the target is N_e and the radius of the flow on the right boundary of the target is r_{rear} , then the total current of electrons is $i = eN_e c \pi r_{rear}^2$, where it is taken into account that electrons move at a speed close to the speed of light. Such a current will produce a magnetic field that reaches a maximum at a distance r_{rear} and equals to

$$B_{cur} = \frac{\mu_0 i}{2\pi r_{rear}} = \frac{1}{2} \mu_0 e N_e c r_{rear} \quad (4)$$

At high current densities, however, the self-interaction of the electron current can no longer be neglected. It will start pinching, which will destroy the simple current structure. In the limiting case of current densities so large that electrons are magnetized by the magnetic fields generated by them, the magnitude of the magnetic field will be limited by the equality of the kinetic pressure of electrons and the magnetic pressure. In this case, the magnitude of the magnetic field can be estimated as follows:

$$B_{sat} = (2\mu_0 N_e T_e)^{1/2}, \quad (5)$$

where T_e is estimated by the expression (2).

Since the electron flow expands as it passes through the target, its radius at the exit of the target will be different from its radius at the moment of generation. If we assume that the radius of the generated beam is approximately equal to the radius of the laser focusing spot r_{spot} , then the radius of the beam at the exit of the target can be determined from a simple geometric equality:

$$r_{rear} = r_{spot} + d \tan \theta \quad (6)$$

The angle θ is difficult to estimate theoretically, but comparison with numerical simulations and experimental results gives good agreement when its value is of the order of $\pi/4$ [25].

The expansion of the beam leads also to a drop in the electron concentration. We can assume that the electron concentration at the moment of generation is approximately

equal to the relativistic critical concentration γN_{cr} , so at the rear side of the target, it will be equal to

$$N_e = N_{cr} \left(1 + a^2\right)^{1/2} \left(\frac{r_{rear}}{r_{spot}}\right)^2. \quad (7)$$

Thus, the values of the generated magnetic fields can be related to the parameters of the incident laser radiation.

With increasing laser intensity, one can expect a transition from low to high electron flux intensity and, consequently, a transition from the model described by the expression (4) to the model described by the expression (5). To verify this, as well as to evaluate how close the field estimates given by these expressions are to the real values, we plot the dependence of the magnetic field obtained in the numerical simulations near the point of electron exit from the target on the laser field intensity and compare them with the predictions of the models. The result is shown in the Figure 2.

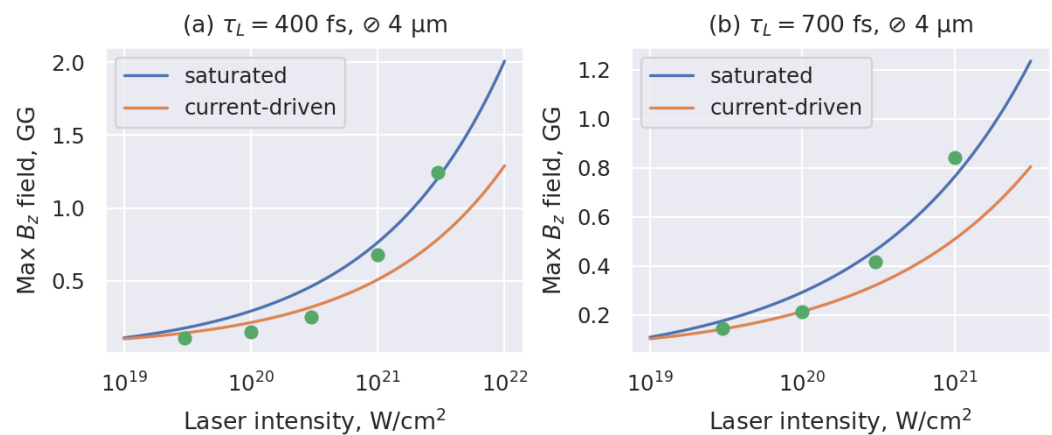


Figure 2. Comparison of the magnetic field magnitude predicted by the models in the unmagnetized case (4) and in the magnetized case (5) with the results of PIC simulations (points) for pulses with durations of (a) 400 fs and (b) 700 fs focused into a 4 μm spot.

Note, first, that the magnetic field values predicted by the models coincide very well with the results of numerical simulations. Second, we can see that, as expected, the model (4) better describes the field at low intensities, and the model (5) at high intensities.

3.2. Modified Mora Model

The transition to the regime in which the electrons in the expanding plasma cloud are magnetized affects the ion acceleration process. At the considered parameters, the typical energies of accelerated protons are 10–100 MeV, i.e., their velocities lie in the range 0.15–0.4 c . In the unmagnetized case, electrons, being ultrarelativistic, easily reach the front of the expanding plasma and, reversed by charge separation forces, begin to perform oscillatory motion throughout the plasma volume, which leads to effective temperature equalization throughout the whole volume. In contrast, in the magnetized case, electrons move along the plasma with the drift velocity caused by the gradient of the magnetic field. The velocity of this drift in a sufficiently large cloud will be lower than the velocity of proton front motion so that the electrons are effectively isolated from the front. Since the intensity of laser radiation in the pulse increases gradually, this leads to the inhomogeneous heating of the plasma cloud as hotter electrons are thrown into the plasma at later time moments. Ions flying at the front of the expanding plasma have the highest energy. Thus, the hottest electrons do not contribute to the acceleration of the most energetic ions, which leads to an effective decrease in the energy achieved by them.

To take this process into account in the above-described Mora model, we propose a simple modification based on the approximation of an instantaneous transition from the unmagnetized state of the plasma to the magnetized state. As a criterion for the transition, we propose to use a comparison of the Larmor radius of the electron R_L to the distance d_f between the front of the accelerated ions and the rear boundary of the target. If the radius R_L for the magnetic field corresponding to the intensity maximum in the laser pulse is larger than the distance d_f at the moment of arrival of the intensity maximum, we will assume that the plasma remains unmagnetized during the whole interaction and the expression (3) remains unchanged. In the opposite case, we should find such a moment of time t_{cr} at which the radius R_L becomes comparable with the distance d_f , and use in the Formula (3) the field amplitude at this moment of time instead of the maximum value.

To estimate the Larmor radius, we will use the magnetic field calculated from one of the models proposed in the previous section. Since they give close values of the field, we can use any of them. In our work, we use the model (5):

$$R_L(t) = \frac{m_e c \gamma_T}{e B_{sat}} = \left(\frac{m_e a(t)}{2 \mu_0 e^2 N_e(t)} \right)^{1/2}, \quad (8)$$

where $\gamma_T = 1 + T_e/m_e c^2 \approx T_e/m_e c^2$ is a gamma factor of a thermal electron, and we use approximation $T_e(t) \approx a(t) m_e c^2$ valid for $a(t) \gg 1$, and $N_e(t)$ is given by (7).

The distance d_f can be estimated from the ion front velocity, determined by the energy of the cutoff ions ε_c , and the time t elapsed since the beginning of the interaction:

$$d_f(t) = ct \left(1 - \left(\frac{m_i c^2}{m_i c^2 + \varepsilon_c(t)} \right)^2 \right)^{1/2}, \quad (9)$$

where $\varepsilon_c(t)$ is determined by (3) with a_{max} being the current laser amplitude $a(t)$ and $\tau_L = t$.

Note that both the radius R_L (8) and the distance d_f (9) depend on the laser amplitude. In this case, at the initial moment of time $T_e = 0$, $d_f = 0$, $R_L \rightarrow \infty$, and later d_f begins to increase (the plasma front begins to move), and R_L decreases (the magnetic field grows), so the problem is reduced to finding such a t_{cr} at which R_L equals to d_f . If there is no such moment of time, it means that the plasma remains unmagnetized the whole time, and one should use the maximum temperature of electrons reached at the moment of time $t = \tau_L/2$.

In practice, however, the equality $R_L = d_f$ turns out to be too coarse a criterion, and for better agreement with the numerical simulation, the introduction of the fitting parameter α is required such that the criterion for the transition from the unmagnetized regime to the magnetized regime is the equality $R_L = \alpha d_f$. As shown below, good agreement in a relatively wide range of interaction parameters is achieved at the value $\alpha = 0.2$.

3.3. PIC Simulations of Ion Energy Scaling

In order to compare the original Mora model with the proposed modification and to evaluate the correctness of the proposed model, a multiparameter numerical simulation is carried out. During this modeling, the dependence of the cutoff energy of the accelerated proton spectrum on the laser intensity is measured for different pulse durations and focusing spot diameters. The results are presented in Figure 3. The theoretical curves for the Mora model and its modification proposed in this work are also given.

Note that, as stated above, a good coincidence in energies requires a multiplication of the value given by the expression (3) by a fitting multiplier of order 1–2. This multiplier is indicated in the corresponding plots and is the same for all intensities. It can also be seen that at high intensities, there is a considerable deviation of the proton cutoff energy

measured in the simulations from the predictions of the Mora model. The deviations begin at intensities at which the transition to the magnetized regime is observed in Figure 2. These deviations are more pronounced for longer pulses, for which the plasma has time to expand to a considerable distance during the interaction. In this case, the modified Mora model gives better agreement with the results of numerical simulations.

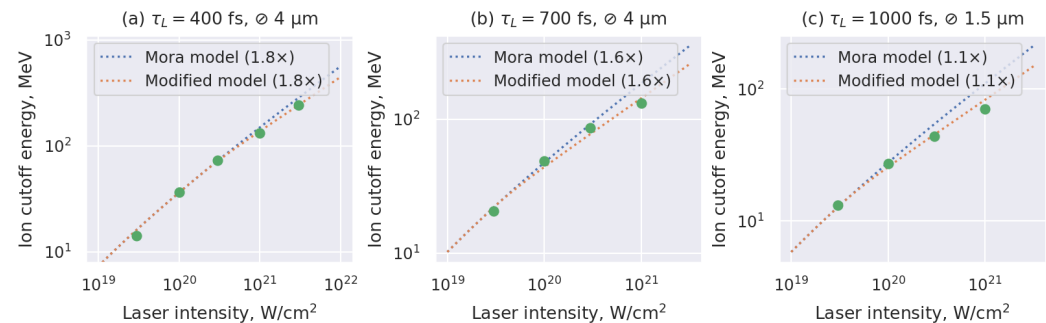


Figure 3. Comparison of the predictions of the original and modified Mora models with PIC simulation results (dots) for pulses (a) of 400 fs duration and 4 μm focal spot, (b) of 700 fs duration and 4 μm focal spot, (c) of 1000 fs duration and 1.5 μm focal spot. Model predictions are multiplied by the fitting multiplier indicated in the legends.

Finally, it should be noted that we do not observe any significant deviation from the Mora model for laser pulse durations less than 400 fs in the investigated intensity range. For short pulses, the accelerating ion front does not have sufficient time to expand, so the self-magnetization is not observed.

4. Conclusions

In this work, we have proposed a modification of the widely used Mora model of ion acceleration in a so-called TNSA regime, in which a plasma expansion is induced by the impact of relativistically intense laser radiation on thin solid-density targets. The modification takes into account the effect of the self-magnetization of electrons in an expanding plasma. Self-magnetization occurs when the plasma cloud size exceeds the Larmor radius of electrons in the toroidal magnetic field self-generated by them. In this case, the velocity of electrons is determined by their drift velocity and becomes less than the velocity of the ion front, where the most energetic ions are located. As a result of self-magnetization, the temperature of electrons ceases to be equalized over the entire volume of the cloud, and the energy of ions at the front is determined not by the temperature of the most energetic electrons generated at the moment of arrival of the maximum intensity of the laser pulse but instead by the temperature of the colder fraction of electrons generated at the moment of the beginning of self-magnetization.

Two models of magnetic field generation have been proposed to estimate the Larmor radius of electrons: in the unmagnetized regime, the cylindrical current model, and in the magnetized regime, the model of magnetic and electron kinetic pressure balance. Both models give values of the generated magnetic fields close to each other.

Comparison of the proposed models with the results of fully kinetic electromagnetic simulations showed good agreement of the magnitude of the generated magnetic field with the cylindrical current model for lower intensities, and at sufficiently high intensities, it is better described by the model of magnetized plasma. At the same time, during the transition from one regime to another, a deviation of the ion energy measured in the simulation from the predictions of the standard Mora model is also observed. A simple modification of the Mora model has been proposed based on an assumption of rapid transition from unmagnetized case to the magnetized one. In the latter, it is assumed

that the ion energy is determined by the temperature of electron fraction generated in the beginning of magnetization regime. Matching the only fitting parameter of the model, which characterizes the ratio of the Larmor radius of electrons to the thickness of the expanding cloud, allows to achieve satisfactory agreement between the proposed modified Mora model and numerical calculations in a relatively wide range of laser pulse duration and intensities.

The proposed model allows us to predict the cutoff energy of the accelerated ion spectrum and can be applied in conditions where electron self-magnetization is important. Numerical simulations show that such self-magnetization is observed for relatively long laser pulses (greater than 400 fs) at intensities around and above 10^{21} W/cm². We did not, however, investigate much higher intensities around and above 10^{22} W/cm², where other physical phenomena such as radiation reaction start to play a role. This could be a possible direction for a future work.

Funding: This research was funded by the Ministry of Science and Higher Education of the Russian Federation, state assignment for the Lobachevsky University of Nizhny Novgorod, Project No. FSWR-2020-0035.

Data Availability Statement: The data presented in this study are available on request from the corresponding author.

Acknowledgments: The simulations were performed on resources provided by the Joint Supercomputer Center of the Russian Academy of Sciences.

Conflicts of Interest: The author declares no conflicts of interest. The funders had no role in the design of the study; in the collection, analyses, or interpretation of data; in the writing of the manuscript; or in the decision to publish the results.

Abbreviations

The following abbreviations are used in this manuscript:

FWHM	Full Width at Half Maximum
PIC	Particle-In-Cell
TNSA	Target Normal Sheath Acceleration

References

1. Borghesi, M. Laser-driven ion acceleration: State of the art and emerging mechanisms. *Nucl. Instrum. Meth. Phys. Res. A* **2014**, *740*, 6–9. [[CrossRef](#)]
2. Bulanov, S.V.; Wilkens, J.J.; Esirkepov, T.Z.; Korn, G.; Kraft, G.; Kraft, S.D.; Molls, M.; Khoroshkov, V.S. Laser ion acceleration for hadron therapy. *Physics-Uspekhi* **2014**, *57*, 1149–1179. [[CrossRef](#)]
3. Ledingham, K.; Bolton, P.; Shikazono, N.; Ma, C.M. Towards Laser Driven Hadron Cancer Radiotherapy: A Review of Progress. *Appl. Sci.* **2014**, *4*, 402–443. [[CrossRef](#)]
4. Bychenkov, V.Y.; Brantov, A.V.; Govras, E.A.; Kovalev, V.F. Laser acceleration of ions: Recent results and prospects for applications. *Physics-Uspekhi* **2015**, *58*, 71–81. [[CrossRef](#)]
5. Schreiber, J.; Bolton, P.R.; Parodi, K. Invited Review Article: “Hands-on” laser-driven ion acceleration: A primer for laser-driven source development and potential applications. *Rev. Sci. Instrum.* **2016**, *87*, 071101. [[CrossRef](#)]
6. Yogo, A.; Arikawa, Y.; Abe, Y.; Mirfayzi, S.R.; Hayakawa, T.; Mima, K.; Kodama, R. Advances in laser-driven neutron sources and applications. *Eur. Phys. J. A* **2023**, *59*, 191. [[CrossRef](#)]
7. Zimmer, M.; Scheuren, S.; Kleinschmidt, A.; Mitura, N.; Tebartz, A.; Schaumann, G.; Abel, T.; Ebert, T.; Hesse, M.; Zähler, S.; et al. Demonstration of non-destructive and isotope-sensitive material analysis using a short-pulsed laser-driven epi-thermal neutron source. *Nat. Commun.* **2022**, *13*, 1173. [[CrossRef](#)]
8. Yogo, A.; Lan, Z.; Arikawa, Y.; Abe, Y.; Mirfayzi, S.; Wei, T.; Mori, T.; Golovin, D.; Hayakawa, T.; Iwata, N.; et al. Laser-Driven Neutron Generation Realizing Single-Shot Resonance Spectroscopy. *Phys. Rev. X* **2023**, *13*, 011011. [[CrossRef](#)]
9. Iwata, N.; Mima, K.; Sentoku, Y.; Yogo, A.; Nagatomo, H.; Nishimura, H.; Azechi, H. Fast ion acceleration in a foil plasma heated by a multi-picosecond high intensity laser. *Phys. Plasmas* **2017**, *24*, 073111. [[CrossRef](#)]

10. Yogo, A.; Mima, K.; Iwata, N.; Tosaki, S.; Morace, A.; Arikawa, Y.; Fujioka, S.; Johzaki, T.; Sentoku, Y.; Nishimura, H.; et al. Boosting laser-ion acceleration with multi-picosecond pulses. *Sci. Rep.* **2017**, *7*, 42451. [\[CrossRef\]](#)
11. Simpson, R.A.; Scott, G.G.; Mariscal, D.; Rusby, D.; King, P.M.; Grace, E.; Aghedo, A.; Pagano, I.; Sinclair, M.; Armstrong, C.; et al. Scaling of laser-driven electron and proton acceleration as a function of laser pulse duration, energy, and intensity in the multi-picosecond regime. *Phys. Plasmas* **2021**, *28*, 013108. [\[CrossRef\]](#)
12. Nakatsutsumi, M.; Sentoku, Y.; Korzhimanov, A.; Chen, S.N.; Buffechoux, S.; Kon, A.; Atherton, B.; Audebert, P.; Geissel, M.; Hurd, L.; et al. Self-generated surface magnetic fields inhibit laser-driven sheath acceleration of high-energy protons. *Nat. Commun.* **2018**, *9*, 280. [\[CrossRef\]](#) [\[PubMed\]](#)
13. Wilks, S.C.; Langdon, a.B.; Cowan, T.E.; Roth, M.; Singh, M.; Hatchett, S.; Key, M.H.; Pennington, D.; MacKinnon, A.; Snavely, R.A. Energetic proton generation in ultra-intense laser-solid interactions. *Phys. Plasmas* **2001**, *8*, 542–549. [\[CrossRef\]](#)
14. Mora, P. Plasma Expansion into a Vacuum. *Phys. Rev. Lett.* **2003**, *90*, 185002. [\[CrossRef\]](#)
15. Robinson, A.P.L.; Foster, P.; Adams, D.; Carroll, D.C.; Dromey, B.; Hawkes, S.; Kar, S.; Li, Y.T.; Markey, K.; McKenna, P.; et al. Spectral modification of laser-accelerated proton beams by self-generated magnetic fields. *New J. Phys.* **2009**, *11*, 083108. [\[CrossRef\]](#)
16. Korzhimanov, A.V. Generation of Cold Magnetized Relativistic Plasmas at the Rear of Thin Foils Irradiated by Ultra-High-Intensity Laser Pulses. *Appl. Sci.* **2021**, *11*, 11966. [\[CrossRef\]](#)
17. Huang, H.; Zhang, Z.M.; Zhang, B.; Hong, W.; He, S.K.; Meng, L.B.; Qi, W.; Cui, B.; Zhou, W.M. Investigation of magnetic inhibition effect on ion acceleration at high laser intensities. *Matter Radiat. Extrem.* **2021**, *6*, 044401. [\[CrossRef\]](#)
18. Arber, T.D.; Bennett, K.; Brady, C.S.; Lawrence-Douglas, A.; Ramsay, M.G.; Sircombe, N.J.; Gillies, P.; Evans, R.G.; Schmitz, H.; Bell, A.R.; et al. Contemporary particle-in-cell approach to laser-plasma modelling. *Plasma Phys. Control Fusion* **2015**, *57*, 113001. [\[CrossRef\]](#)
19. Surmin, I.A.; Bastrakov, S.I.; Efimenko, E.S.; Gonoskov, A.A.; Korzhimanov, A.V.; Meyerov, I.B. Particle-in-Cell laser-plasma simulation on Xeon Phi coprocessors. *Comput. Phys. Commun.* **2016**, *202*, 204–210. [\[CrossRef\]](#)
20. Gurevich, A.V.; Pariiskaya, L.V.; Pitaevskii, L.P. Self-similar motion of rarefied plasma. *Sov. Phys. JETP* **1966**, *22*, 449–454.
21. Mora, P.; Pellat, R. Self-similar expansion of a plasma into a vacuum. *Phys. Fluids* **1979**, *22*, 2300–2304. [\[CrossRef\]](#)
22. Dorozhkina, D.S.; Semenov, V.E. Exact Solution of Vlasov Equations for Quasineutral Expansion of Plasma Bunch into Vacuum. *Phys. Rev. Lett.* **1998**, *81*, 2691–2694. [\[CrossRef\]](#)
23. Kluge, T.; Cowan, T.; Debus, A.; Schramm, U.; Zeil, K.; Bussmann, M. Electron Temperature Scaling in Laser Interaction with Solids. *Phys. Rev. Lett.* **2011**, *107*, 205003. [\[CrossRef\]](#) [\[PubMed\]](#)
24. Daido, H.; Nishiuchi, M.; Pirozhkov, A.S. Review of laser-driven ion sources and their applications. *Rep. Prog. Phys.* **2012**, *75*, 056401. [\[CrossRef\]](#) [\[PubMed\]](#)
25. Macchi, A.; Borghesi, M.; Passoni, M. Ion acceleration by superintense laser-plasma interaction. *Rev. Mod. Phys.* **2013**, *85*, 751. [\[CrossRef\]](#)

Disclaimer/Publisher’s Note: The statements, opinions and data contained in all publications are solely those of the individual author(s) and contributor(s) and not of MDPI and/or the editor(s). MDPI and/or the editor(s) disclaim responsibility for any injury to people or property resulting from any ideas, methods, instructions or products referred to in the content.